LIDAR- and non-LIDAR-based canopy parameters to estimate the leaf area in fruit trees and vineyard

Sanz, R.[a,*], Llorens, J.[a], Escolà, A.[a], Arnó, J. [a], Planas, S.[a], Román C.[a], Rosell-Polo, J.R.[a]

[a] Department of Agricultural and Forest Engineering, Research Group in AgroICT and Precision Agriculture, University of Lleida–Agrotecnio Center, Rovira Roure, 191, Lleida, Spain

* Corresponding author at: Department of Agricultural and Forest Engineering, Research Group in AgroICT and Precision Agriculture, University of Lleida–Agrotecnio Center, Rovira Roure, 191, Lleida, Spain.
E-mail address: rsanz@eagrof.udl.cat (Sanz, R.).

Abstract

This paper is based on two initial hypotheses, firstly, it is proposed that the vegetation volume obtained with a LIDAR-based system or tree row LIDAR volume (TRLV) has a high correlation with the leaf area (LA). Secondly, it is proposed that the projected outer surface or projected tree row surface (PTRS), also LIDAR-based, is linearly related with the LA. The verification of these two hypotheses corresponds to the first two objectives of this work. The third objective is to propose an alternative method, without using LIDAR sensors, simpler and more economical, for *in situ* LA evaluation.

To achieve these objectives a total of 17 blocks of pear, 14 of apple and 26 of vine, in different phenological states, were LIDAR scanned and subsequently manually defoliated. After the field and calculation work, the TRLV and LA were compared. The logarithmic regressions obtained had high correlations. For apple and pear trees the equations are practically the same with R^2 of 0.85 and 0.84, respectively. The equation corresponding to vines is somewhat different and has an R^2 of 0.86. The regression without species differentiation is $3.66\ln(x)+9.65$ with $R^2=0.90$.

Based on the TRLV, the front and top projected surface areas of each block were then obtained and, using these variables, the PTRS. The linear regressions obtained between PTRS and LA have high correlations with R^2 of 0.88, 0.85 and 0.80 for apple trees, pear trees, and vineyard respectively. The three crops show very similar behavior. The straight lines are very close, with very similar slopes. With no species differentiation the linear regression model is $y = 1.47x - 1.18$ with $R^2=0.93$.

The starting point of the third objective is to obtain the projected surfaces, frontal and top, without using a LIDAR sensor. These surfaces are not as precise as those obtained with LIDAR and for this reason they are referred to as "estimated" projected surfaces. To calculate the estimated PTRS without a LIDAR sensor, the height and depth of the vegetation are measured with a tape measure. It is also necessary to make a visual estimation of the frontal gap-fraction. For this, a training method with known gap-fraction pictograms is proposed. The final results with this non-LIDAR method are very similar to those obtained with LIDAR. This method, although it needs human intervention, is simple, easy, economical and precise for *in situ* LA estimation.

Keywords: LIDAR, LAI, Vegetation volume, Projected surface, Fruit tree, Gap-fraction.

Highlights:

- The regression model between leaf area and LIDAR-volume is highly significant
- The regression model between leaf area and projected outer surface is highly significant
- Point estimation of leaf area *in situ* is feasible based on height and gap fraction estimation
- Variables which do not take into consideration the gap fraction performed worse in explaining leaf area

1. Introduction

Determination of leaf area (LA) in fruit and vine cultivation is an important but difficult task. Important, because leaves are intrinsically related to evapotranspiration, radiation interception and CO_2 fixation (Hernandez-Santana et al., 2017), and difficult, because of the huge number of leaves and the complexity of the three-dimensional structure of the canopies of fruit trees and vines. It is also difficult to establish the necessary accuracy because it depends on other variables. Quick determinations with errors under 10% are a good starting point. Numerous research studies have required LA determination or estimation in fields such as irrigation (Du et al., 2017; Pereira et al., 2007), fertilization (Fernández et al., 2008), pruning (Ballesteros et al., 2015; Palmer et al., 1992), tree training (Kliewer and Dokoozlian, 2005), or the application of phytosanitary products (Arnó et al., 2015; Pascuzzi et al., 2017; Planas et al., 2013; Siegfried et al., 2007). All of these practices are related to canopy management, a key factor for plantation yield optimization (Cohen et al., 2005).

A review is conducted in Jonckheere et al., (2004) of different methods, both direct and indirect, for determination or estimation of LA. The direct methods are characterized by directly measuring the leaf surface area and the indirect methods by using other parameters which are related to LA but easier to obtain. The former methods are more precise, but entail a high cost in terms of labor and time, often making them unfeasible for commercial purposes. Nonetheless, they are indispensable for the validation and/or calibration of the indirect methods (Doring et al., 2014; Poblete-Echeverría et al., 2015). These latter methods are characterized by their rapidity and the fact that they can often be automated (Fuentes et al., 2014; Mora et al., 2016), making them suitable for the measurement of larger-sized areas. Many of these methods are based on differentiating between green and non-green areas (Diago et al., 2012), The latter are basically the woody material, fruit, flowers and gaps through which light passes. Many of the methods are based on quantification of the light that passes through the gap fraction in order to estimate the green fraction (De Bei et al., 2016; C. Liu et al., 2013). It is also important to bear in mind that, normally, distribution of the green and gap fraction is projected and analyzed in the horizontal plane of the ground, as for example, in a forest environment (Chianucci et al., 2014) or in extensive agricultural crops (Fang et al., 2014; J. Liu et al., 2013). In contrast, there are other environments, no less important, like intensive fruit growing, where it is more interesting to project and analyze the green and gap fraction in a vertical plane since, normally, the height of the crop is greater than its thickness. Due to this arrangement, in general, the gap fraction is larger and easier to measure from a

frontal view than from a top view perspective. Amongst other methods, ultrasound sensors are being used for the characterization of such crops (Escolà et al., 2011; Llorens et al., 2011a), as well as LIDAR sensors (Auat Cheein et al., 2015; Pfeiffer et al., 2018; Rosell and Sanz, 2012) The latter are becoming more commonly used as their price gradually falls and the features they offer increase. LIDAR sensors have been used for a number of years for 3D vegetation modelling, generating three-dimensional point clouds (Arnó et al., 2013; Llorens et al., 2011b; Moorthy et al., 2008). Complex geometrical variables can be obtained based on the use of these point clouds, including volumes (Auat Cheein et al., 2015; Escolà et al., 2017; Rosell Polo et al., 2009; Sanz et al., 2013) and LA-related surface areas (Arnó et al., 2013; Llop et al., 2016; Méndez et al., 2013; Sanz-Cortiella et al., 2011). Below, a description is given of the initial hypotheses and aims of the present study.

Hypothesis and Objectives

This present study is based on two initial hypotheses. Firstly, it is proposed that the vegetation volume obtained with a LIDAR-based system or tree row LIDAR volume (TRLV) has a high correlation with the LA. Secondly, it is proposed that the projected outer surface or projected tree row surface (PTRS) is linearly related with the LA.

The objectives considered in this work are as follows:

- Study of the relationship between TRLV and LA in apple tree orchards (*Malus communis* L.), pear tree orchards (*Pyrus communis* L.), and vineyards (*Vitis vinifera* L.).

- Study of the relationship between PTRS and LA in the same crops as above.

- To propose an alternative method, without using LIDAR sensors, simpler and more economical, for *in situ* LA evaluation.

2. Materials and methods

2.1. Location and main characteristics of the tested orchards/vineyards

The tests were carried out at six sites in Catalonia, Spain (Table 1), Gimenells, Mollerussa, Alfarrás, Caldes de Montbui, Raimat, and Espiells, over the course of three years between April and August. The crops studied were: apple trees (*Malus communis* L. 'Red Chief', 'Golden', 'Fuji', 'Gala', and 'Gala Brookfield'), pear trees (*Pyrus communis* L. 'Conference' and 'Blanquilla') and vines (*Vitis vinifera* L. 'Cabernet Sauvignon', 'Merlot', 'Tempranillo' and 'Syrah'). A total of 17 blocks of pear, 14 of apple and 26 of vine, in different phenological states (BBCH scale, Table 1), were LIDAR scanned and subsequently manually defoliated (Fig. 1). Block lengths ranged between 1.5 and 3.15 m, heights between 0.84 and 4 m, and row depths between 0.31 and 2.6 m. Visual estimation was also performed of the percentage of frontal gaps (Table 1). Altogether, 57 blocks were analyzed. Once in the laboratory, a planimeter (Delta-T Devices Ltd., Cambridge, UK) was used in combination with a gravimetric method, correlating fresh weight of leaves and leaf area (m^2). Only one of the leaf faces was

considered for leaf area measurement. The planimeter consists of two different parts, a conveyor belt and an image analysis system.

The blocks were chosen based on variability in terms of age, size, phenological stage and training system (Fig. 1 and Table 1).

Table 1
Tests conducted. Principal data.

Crop (Village) / Block	Test date (d/m)	BBCH scale	Length (m)	Height (m)	Depth (m)	Row Spacing (m)	Frontal Gaps (%)
Pear *Conference* (Gimenells) / BI	20/05	71-75	1.50	3.00	1.05	4.00	20
Pear *Conference* (Gimenells) / BII	16/07	76-89	1.50	3.00	1.30	4.00	10
Pear *Conference* 1-axis (Mollerussa) / BI	20/05	71-75	2.93	3.10	1.70	4.00	25
Pear *Conference* 1-axis (Mollerussa) / BII	14/07	76-89	3.12	3.30	1.55	4.00	25
Pear *Conference* 2-axis (Mollerussa) / BI	20/05	71-75	2.00	3.80	1.15	4.00	10
Pear *Conference* 2-axis (Mollerussa) / BII	14/07	76-89	1.85	3.70	0.95	4.00	10
Pear *Blanquilla* (Gimenells) / BI	20/05	71-75	2.00	3.15	1.90	4.00	20
Pear *Blanquilla* (Gimenells) / BII	16/07	76-89	2.00	3.10	1.70	4.00	15
Pear *Blanquilla* (Gimenells) / BIII	16/06	76-89	1.90	2.90	1.40	4.00	10
Pear *Blanquilla* (Alfarrás) / BI	18/04	71-75	2.00	2.50	0.85	4.50	50
Pear *Blanquilla* (Alfarrás) / BII	18/04	71-75	2.00	2.50	0.90	4.50	40
Pear *Blanquilla* (Alfarrás) / BIII	03/05	71-75	2.00	2.55	0.95	4.50	50
Pear *Blanquilla* (Alfarrás) / BIV	03/05	71-75	2.00	2.50	1.00	4.50	40
Pear *Blanquilla* (Alfarrás) / BV	02/06	71-75	2.00	2.60	1.10	4.50	20
Pear *Blanquilla* (Alfarrás) / BVI	02/06	71-75	2.00	2.60	1.28	4.50	20
Pear *Blanquilla* (Alfarrás) / BVII	25/07	76-89	2.00	2.60	1.10	4.50	30
Pear *Blanquilla* (Alfarrás) / BVIII	25/07	76-89	2.00	2.60	1.13	4.50	20
Apple *Red Chief* (Gimenells) / BI	26/05	71-75	1.60	3.40	2.60	4.00	0
Apple *Red Chief* (Gimenells) / BII	14/07	76-89	1.50	3.40	2.60	4.00	0
Apple *Golden* (Gimenells) / BI	26/05	71-75	1.52	3.40	1.60	4.00	20
Apple *Golden* (Gimenells) / BII	14/07	76-89	1.49	2.40	1.50	4.00	5
Apple Gala Brookfield 1-axis (Mollerussa) / BI	20/05	71-75	2.70	2.90	1.40	4.00	50
Apple Gala Brookfield 1-axis (Mollerussa) / BII	14/07	76-89	2.30	3.40	1.25	4.00	50
Apple *Fuji* 1-axis (Mollerussa) / BI	20/05	71-75	2.80	3.20	1.70	4.00	40
Apple *Fuji* 1-axis (Mollerussa) / BII	14/07	76-89	2.65	3.35	1.60	4.00	50
Apple *Fuji* wall (Mollerussa) / BI	20/05	71-75	2.75	3.07	0.95	4.30	40
Apple *Fuji* wall (Mollerussa) / BII	14/07	76-89	2.62	3.10	0.85	4.30	40
Apple *Gala Brookfield* wall (Mollerussa) / BI	20/05	71-75	3.03	3.40	0.65	4.50	60
Apple *Gala Brookfield* wall (Mollerussa) / BII	14/07	76-89	2.78	3.00	0.55	4.50	60
Apple *Gala* 1-axis (Mollerussa) / BI	20/05	71-75	3.04	3.45	1.65	4.00	15
Apple *Gala* 1-axis (Mollerussa) / BII	14/07	76-89	3.15	4.00	1.68	4.00	20
Vineyard *Cabernet* (Caldes de Montbui) / BI	03/06	71-89	2.00	1.08	0.42	3.00	50
Vineyard *Cabernet* (Caldes de Montbui) / BII	03/06	71-89	2.00	1.36	0.35	3.00	60
Vineyard *Cabernet* (Caldes de Montbui) / BIII	26/07	71-89	2.00	1.50	1.02	3.00	15
Vineyard *Merlot* (Caldes de Montbui) / BI	03/06	71-89	2.00	1.06	0.31	3.00	50
Vineyard *Merlot* (Caldes de Montbui) / BII	03/06	71-89	1.90	0.84	0.44	3.00	25
Vineyard *Merlot* (Caldes de Montbui) / BIII	30/06	71-89	2.00	1.44	0.50	3.00	40
Vineyard *Merlot* (Caldes) / BIV	26/07	71-89	2.00	1.38	0.60	3.00	35
Vineyard *Merlot* (Raimat) / BI	10/05	55-69	2.00	1.22	0.36	3.00	60
Vineyard *Merlot* (Raimat) / BII	10/05	55-69	2.00	1.20	0.34	3.00	50
Vineyard *Merlot* (Raimat) / BIII	06/06	71-89	2.00	1.24	0.58	3.00	25
Vineyard *Merlot* (Raimat) / BIV	06/06	71-89	2.00	1.70	0.61	3.00	35
Vineyard *Merlot* (Raimat) / BV	07/07	71-89	2.00	1.62	0.80	3.00	25
Vineyard *Merlot* (Raimat) / BVI	07/07	71-89	2.00	1.62	0.98	3.00	30
Vineyard *Merlot* (Raimat) / BVII	24/08	71-89	2.00	1.42	0.80	3.00	30
Vineyard *Merlot* (Raimat) / BVIII	24/08	71-89	2.00	1.64	0.71	3.00	40
Vineyard *Syrah* (Raimat) / BI	24/07	71-89	1.90	1.35	0.58	3.00	15
Vineyard *Syrah* (Raimat) / BII	24/07	71-89	1.96	1.46	0.67	3.00	25
Vineyard *Syrah* (Raimat) / BIII	24/07	71-89	2.12	1.46	0.60	3.00	30
Vineyard *Syrah* (Raimat) / BIV	24/07	71-89	1.86	1.32	0.50	3.00	40
Vineyard *Syrah* (Raimat) / BV	24/07	71-89	2.06	1.46	0.68	3.00	15
Vineyard *Cabernet* (Espiells) / BI	09/06	71-89	1.82	1.38	0.62	3.00	40

Vineyard *Cabernet* (Espiells) / BII	02/07	71-89	2.02	1.32	0.81	3.00	25
Vineyard *Cabernet* (Espiells) / BIII	21/07	71-89	2.02	1.53	0.59	3.00	45
Vineyard *Tempranillo* (Espiells) / BI	09/06	71-89	1.38	1.02	0.44	3.00	45
Vineyard *Tempranillo* (Espiells) / BII	02/07	71-89	2.71	1.53	0.59	3.00	25
Vineyard *Tempranillo* (Espiells) / BIII	21/07	71-89	2.54	1.60	0.61	3.00	35

(a) (b) (c)

Fig. 1. Three of the 57 defoliated blocks. A) Vineyard *Cabernet* (Espiells), 09/06 b) Pear *Conference* 1-axis (Mollerussa), 14/07 c) Apple *Gala Brookfield* wall (Mollerussa), 20/05. The white background is used to photographically isolate the block.

2.2. Description of the measurement system

A Sick LMS200 (SICK AG, Düsseldorf, Germany) LIDAR sensor was used in the 3D measurement system. This sensor measures distances in a single plane, with an accuracy of ± 1.5 cm in a 0 to 8 m range. The maximum angular range is 0-180°. The angular resolutions used were 1° and 0.5°. Laser emission wavelength was 905 nm (near infrared) and Class 1 eye-safe. Communication between sensor and PC used the RS-232 protocol at a speed of 38400 bits per second. A total of 1700 measurements of distance per second were obtained with this configuration. The scanning plane of the tests was vertical and perpendicular to the vegetation. The beam directions of 0° and 180° were both vertical, pointing upwards and downwards, respectively (Fig. 2). Each block was scanned twice, once on each side (left and right side), following rectilinear trajectories with a constant speed of between 1.0 and 2.1 km/h. The two point clouds, one from each scan, were subsequently registered into a single point cloud. In the tests, no geolocation receiver (GNSS) was used. Four reference plane elements, two on each side of the row, with perfectly known position and dimensions, were used to facilitate the centimeter-registration process (Rosell et al., 2009).

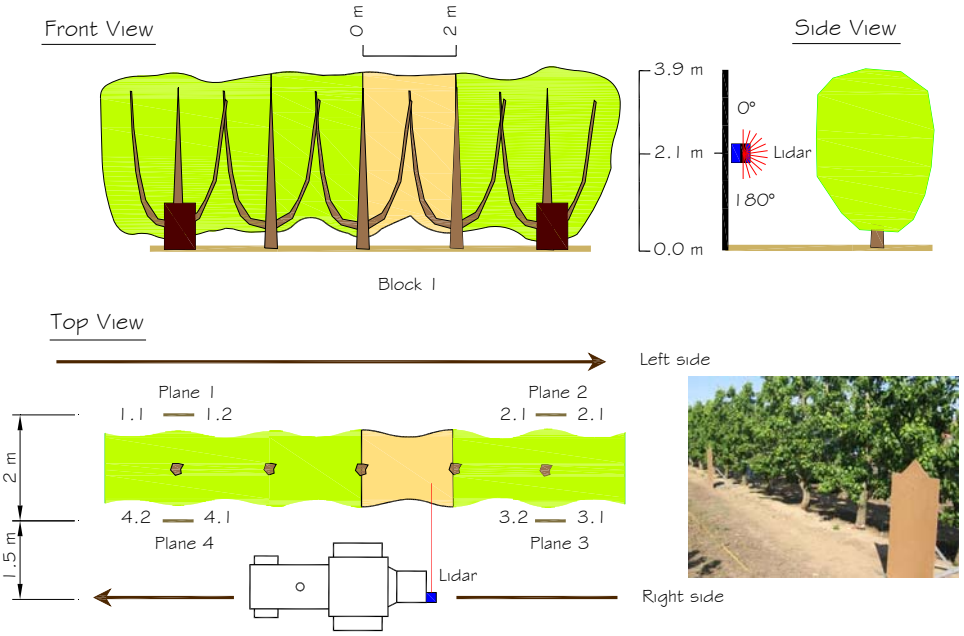

Fig. 2. Schematic description of the tests. Photograph of the two reference planes on one side (adapted from Sanz-Cortiella et al., 2011).

The theoretical point spacing in the frontal mid-plane of vegetation at the height of the LIDAR sensor have horizontal separations of between 18 and 89 mm, though only in 5 blocks did these exceed 60 mm. Vertically, separations ranged between 29 and 43 mm. These ranges depended principally on the speed at which the sensor advanced, on the distance between the sensor and the vegetation and on the angular resolution configuration. The point clouds that were generated do not allow differentiation between individual leaves, but do show in good detail the shape and size of the irregularities of the walls of vegetation.

2.3. Leaf Area estimation process

This section is divided into two subsections. The first one explains the LIDAR-based variables that were used to estimate LA. These variables are fundamental for the first two objectives of this work. The second subsection, and related to the third objective, explains the non-LIDAR-based variables for *in situ* LA estimation.

Regarding the units in which all these variables have been expressed, in the agricultural environment it is very common to express them by unit of area, e.g. l/ha, kg/ha, €/ha, but in this work the variables have been expressed per unit of length. For this reason, the value of the variables of each block has been divided by its length in m, leaving the variables referred to a linear meter (/m) of fruit/vineyard row.

2.3.1 Leaf Area estimation using LIDAR-based variables

After the accurate registration of the point clouds, the variables that subsequently correlated with the LA were calculated. First the TRLV was graphically and numerically (m^3/m) obtained (Fig. 3) (Sanz et al., 2013). The mechanism used to obtain the TRLV was based on the intersection of two solids. Each solid is equivalent to the shadow space which the laser emission of the LIDAR generates. All the sensor generated points were used to obtain this volume, including both, those that strike the vegetation, as well as those that pass through the gaps. Data about the gaps is vital in order to obtain a better representation of the vegetation.

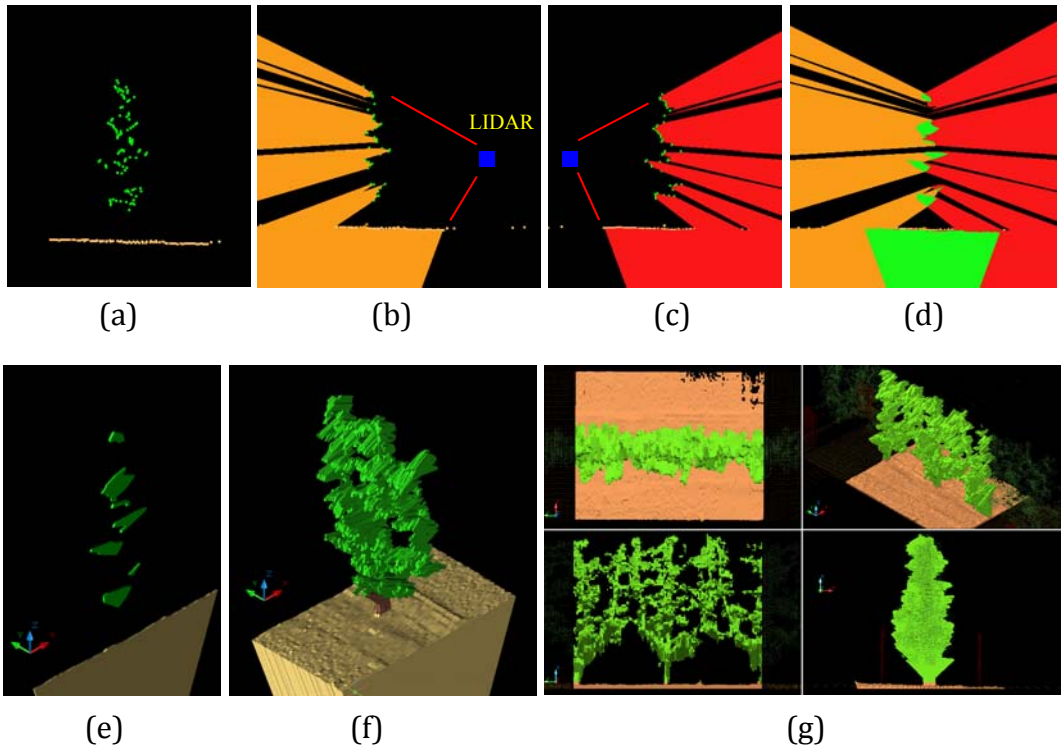

Fig. 3. Graphic explanation of the process followed for the generation of the TRLV. (a) Point cloud of a very short section of vegetation, just 0.05 m long. (b) Solid generated from the points obtained from the right-hand side scanning (in orange). (c) Solid generated from the points obtained from the left-hand side scanning (in red). (d) Result of the intersection (in green) of the (b) and (c) solids. (e) Isometric view of the solid generated of a 0.05 m long section of vegetation. f) Isometric view of the TRLV of a 2 m long section of vegetation. g) Top (XY), frontal (YZ), lateral (XZ) and isometric view of the TRLV of a 4 m long section of vegetation (adapted from Sanz et al., 2013).

The other variables that correlated with the LA were the projected flat surfaces of the vegetation. With the TRLV and using CAD software (Autocad® version 2014, Autodesk, Inc., San Rafael, CA, USA), the flat frontal projected surface (PFS) and the flat top projected surface (PTS) were then graphically and numerically (m^2/m) obtained from all the blocks. An example of TRLV and its projections, PFS and PTS, are shown in Fig. 4c. It can be seen that the frontal and rear projections are coincident, as are the top and lower. Fig. 4a shows the rectangle ($l \times h$) occupied by the PFS and the frontal gaps. In Fig. 4b the PTS and its equivalent rectangle surface are shown. In the 57 analyzed blocks, very few and insignificant gaps were found in the PTS. For this reason, gaps were not taken

into account in this projection. Combinations of the PFS and the PTS were analyzed to compare the regression models. The first combination, projected tree row surface (PTRS), is defined as the outer surface area, comprised of the four outer faces (4F), frontal, rear, top and lower. PTRS (m^2/m) is calculated as shown in Eq.(1). The second combination is based on the fact that the lower part of the vegetation is the least illuminated, therefore the lower face was discarded and the combination of the three remaining faces (3F) frontal, rear and top was also studied. Finally, the regression models with the frontal face and with the top face were analyzed separately.

$$PTRS = 2PFS + 2PTS \quad (1)$$

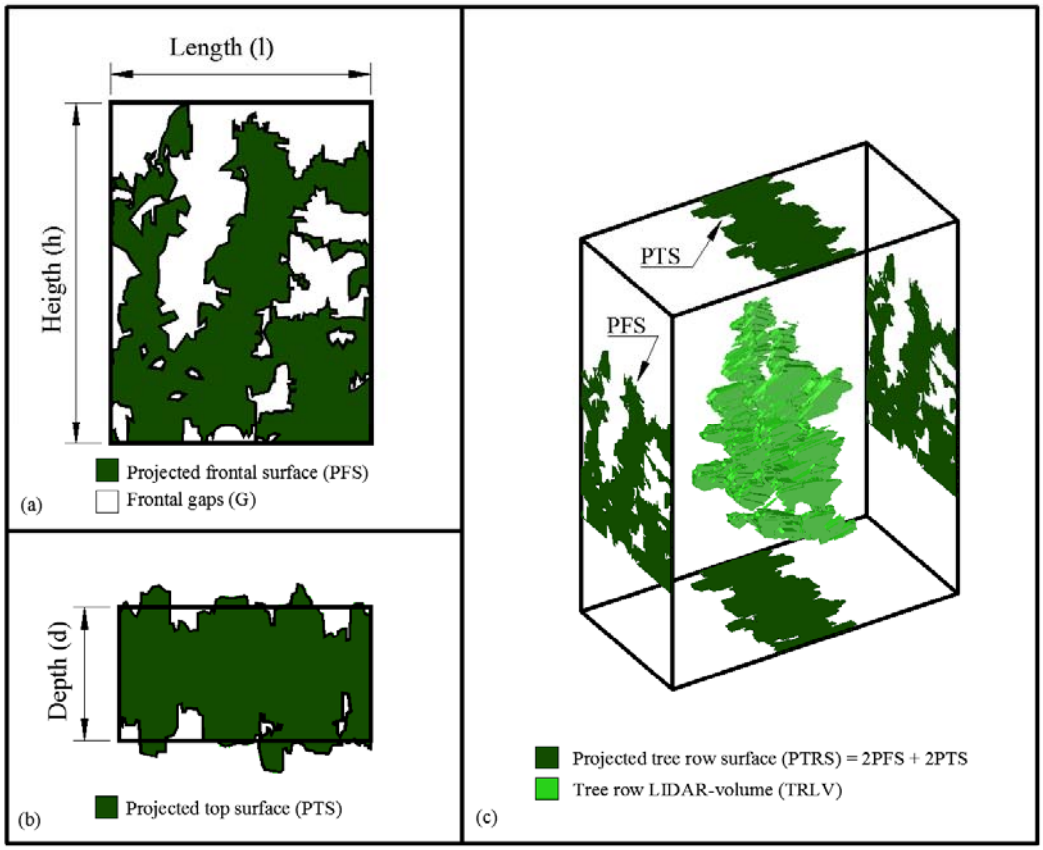

Fig. 4. Example of TRLV and its projections, PFS and PTS. (a) Rectangular surface occupied by the PFS and the frontal gaps. (b) PTS and its equivalent rectangle surface. (c) 3D view of the TRLV, PFS and PTS.

2.3.2 Leaf Area estimation without using LIDAR-based variables

The third objective of this work is to provide an alternative method of LA estimation, without using the LIDAR sensor. The starting point of this new method is to obtain the flat projected surfaces, frontal and top, without using a LIDAR sensor. These surfaces will not be as precise as those obtained with LIDAR and for this reason they are referred to as "estimated" projected flat surfaces. The name of the new variables is the same as those based on the LIDAR sensor, but preceded by an E. The new variables are the following; estimated projected front surface (EPFS), estimated projected top surface

(EPTS) and estimated projected tree row surface (EPTRS). The EPTRS (m^2/m), like the PTRS, is defined as the outer surface area, comprised of the four outer faces, frontal, rear, top and lower. EPTRS is calculated as shown in Eq.(2)

$$EPTRS = 2EPFS + 2EPTS \quad (2)$$

To obtain the EPFS (m^2/m) (Eq.(3)) in field, the following is proposed: analyze the frontal rectangle which contains the vegetation to be studied (Fig. 4a), measure its height (h) with a measuring tape and visually estimate the percentage of gaps or gap fraction (G). The length of the rectangle (l) is both multiplied and divided and therefore is cancelled out.

$$EPFS = (l \times h) \times (1 - G/100) / l \quad (3)$$

To obtain the EPTS (m^2/m) (Eq.(4)) in field, it is proposed to measure the maximum depth at several points, with a measuring tape, and calculate its average (d) (Fig. 4b). The length of the rectangle (l) is both multiplied and divided and, therefore, is again not taken into account.

$$EPTS = (l \times d) / l \quad (4)$$

At the time the field tests were carried out, there was no plan to search for an alternative method to using the LIDAR and for this reason there was no manual measurement of the mean maximum depth nor estimation of the percentage of gaps of the scanned blocks. These two variables were obtained *a posteriori* using the LIDAR-generated point clouds. To obtain the gap fraction, a collaborator in the research study, after training sessions using pictograms (Fig. 5), visually estimated the G (Table 1) of all the blocks. Also based on the LIDAR-generated point clouds, 5 equidistant measurements of depth were averaged to obtain the mean maximum depth (d) of each block (Table 1).

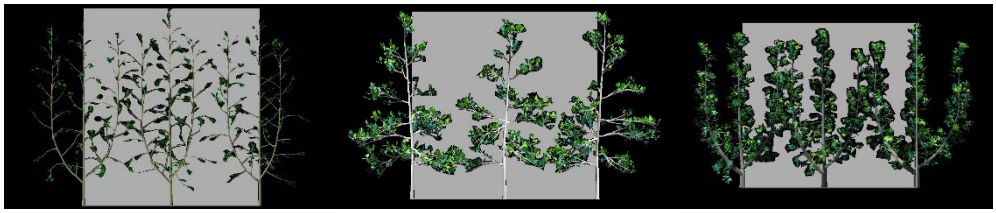

80% 70% 51%

40% 36% 31%

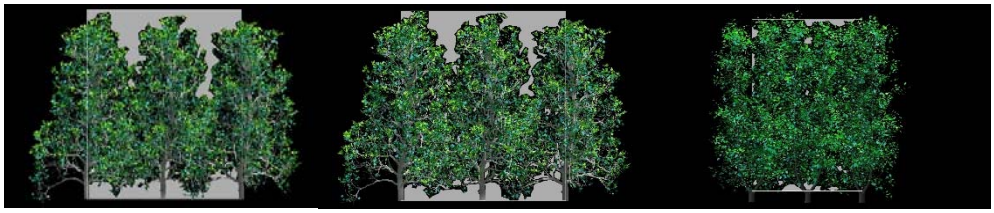

20% 16% 3%

Fig. 5. Examples of pictograms with known percentage of frontal gaps for visual training in gaps estimation.

A very important variable in fruit cultivation is the leaf area index (LAI), the one-sided green leaf area per unit ground surface area (m^2/m^2). Currently in the agricultural environment, on a practical level, the use of LAI is much more frequent than LA per linear meter of tree row. Its calculation, based on LA (m^2/m), is simple and is expressed in Eq.5, where RS (m) is the distance between tree rows or row spacing (Table 1):

$$LAI = LA / RS \quad (5)$$

Given that the variable EPFS is also easy to obtain and, as will subsequently be seen, has a high correlation with LA, finally an analysis is made of the correlation between EPFS and LAI. This analysis aims to show that it is easy to make a good estimate "in situ" of LAI.

The results of the different procedures proposed for LA estimation are ordered beginning with the most accurate and laborious methods and finishing with the least accurate but simplest ones. Firstly, a study is undertaken of the correlation between the TRLV and the LA (section 3.1), and then the correlation between the projected surfaces (PTRS, PFS and PTS) and the LA (section 3.2). This is followed by the proposal of simpler solutions which do not depend on the use of a LIDAR sensor (section 3.3). In this section the following correlations are analyzed: PTRS/EPTRS, EPTRS/LA, EPFS/LA and height/LA. Finally, a global analysis is made based on the root mean square errors (RMSE) of all the regression models obtained (section 3.4).

3. Results and discussion

3.1. Estimation of the LA from the TRLV

After the field and calculation work, the TRLV and LA were compared. The logarithmic regressions obtained had a high correlation, with *p*-value < 0.001, as can be seen in Fig. 6. The significance codes used in this article are as follows: 0 '***' 0.001 '**' 0.01 '*' 0.05 '.' 0.1 ' ' 1. For apple and pear trees the equations are practically the same with R^2 of 0.85 and 0.84, respectively. The equation corresponding to vines is somewhat different and has an R^2 of 0.86. Despite this difference, the three equations overlap and this seems to indicate that the three species behave similarly in terms of the correlation between these two variables. The regression without species differentiation is 3.66ln(x)+9.65 *** with R^2=0.90 and RMSE=1.26. This is not plotted because it is coincident on the other three regressions.

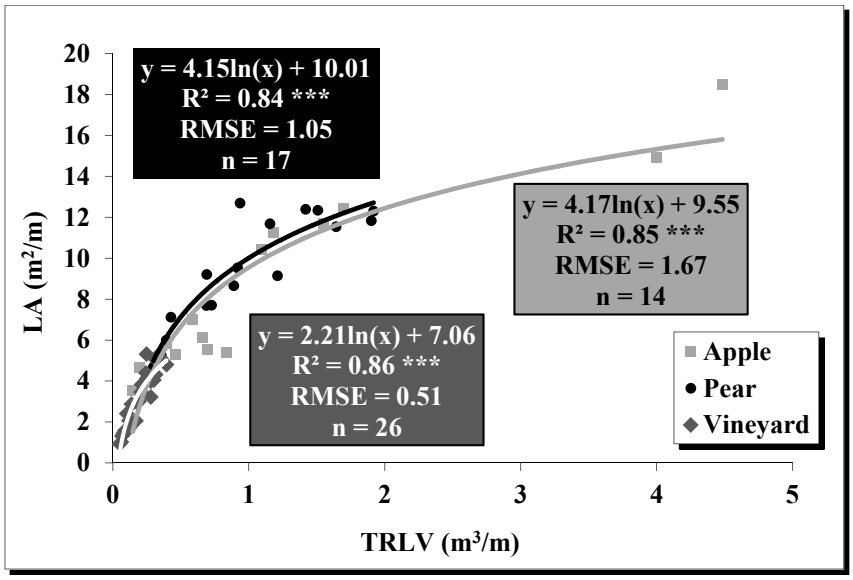

Fig. 6. Scatter diagram and logarithmic regression of the relationship between the TRLV and LA for vine, pear and apple tree blocks, fitted independently.

A more detailed analysis of the results for vine is shown in Fig.7, given that this crop had the most blocks, 26 in total. High correlations can be observed, with Cabernet the variety with lowest leaf density (LA/TRLV) and Tempranillo the highest. A certain degree of prudence is required in this respect as the number of samples per variety is small, especially when considering only 3 blocks of Tempranillo have been analyzed.

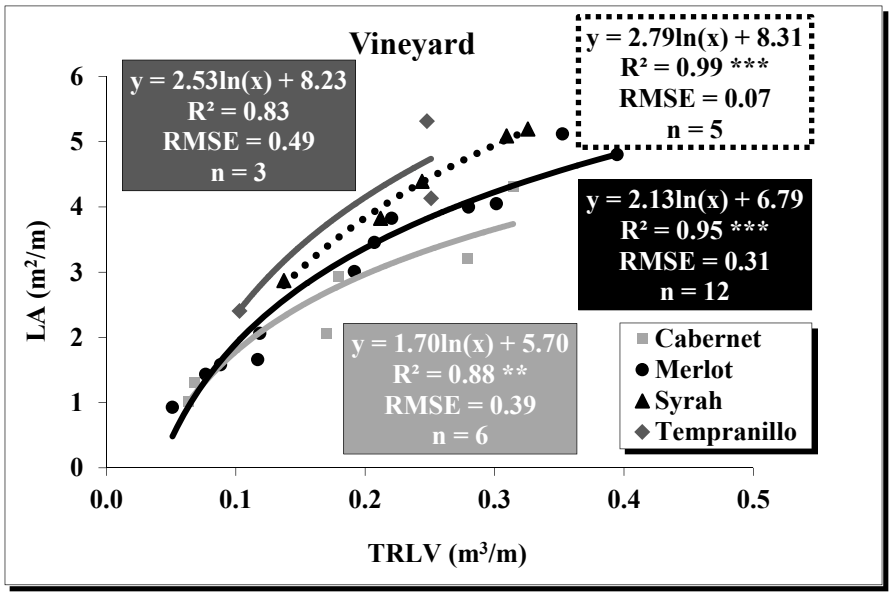

Fig. 7. Scatter diagram and logarithmic regression of the relationship between the TRLV and LA for Cabernet, Merlot, Syrah and Tempranillo vines, fitted independently.

The curves of Figs. 6 and 7 show that TRLV increases faster than LA. This can be explained by the tendency of the plants to position leaves mainly in the outer part of the

canopy so that they have greater access to light. The main drawback to this LA estimation method is the need to use a LIDAR-based system and to use a semi-automated post-processing system to transform the point cloud into TRLV. The first hypothesis, which assumes that the TRLV is a good variable for LA estimation, was confirmed by these results.

3.2. Estimation of the LA from the projected surfaces

Based on the TRLV, the PFS and PTS were then obtained and, using these variables, the PTRS. Firstly, an analysis was made of the correlation between PTRS and LA. It can be seen (Fig.8 and Table 2) that there are very high correlations with *p*-value < 0.001. As in Fig.6, the three crops show very similar behavior. The straight lines are very close, with very similar slopes. With no species differentiation, an R^2=0.93 was obtained with an RMSE=1.10 m^2/m. It can also be seen that the models give a PTRS >0 when LA=0. This is consistent, as in the absence of leaves there still remains the structural part of trunk and branches, and a good indication of the consistency of these models. This result is very interesting given that it is based on 57 blocks of widely varying characteristics and scenarios which give a similar response in terms of leaf arrangement for the capture of light. When the regression lines are forced to pass through the origin, the RMSE logically increases a little, but the interpretation of the results is simplified. In this case, the slopes of 1.26, 1.35 and 1.14 (Table 2) reveal that the leaves partly overlap, with leaf surface area larger than the PTRS. The biggest overlap corresponds to pear trees and the lowest to vines.

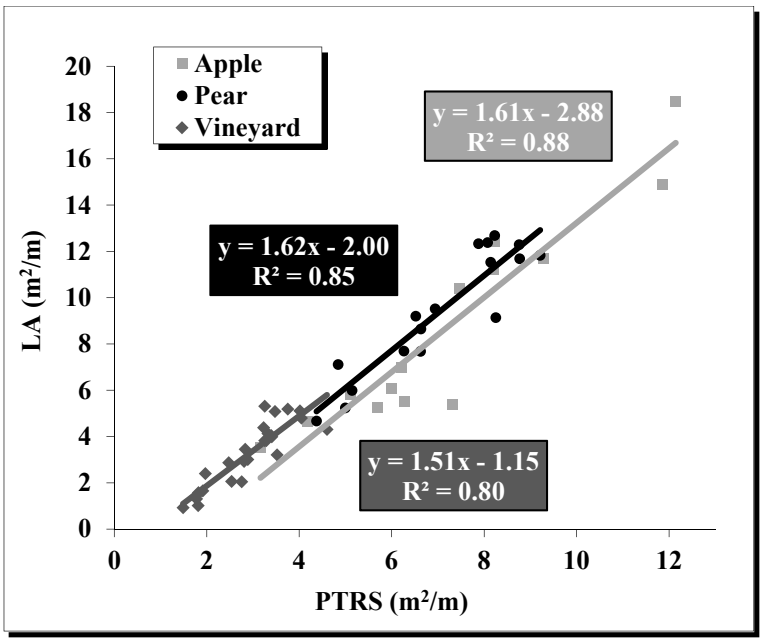

Fig. 8. Scatter diagram and linear regression of the relationship between the PTRS and LA for vine, pear and apple tree blocks, fitted independently.

Table 2

Linear regression and linear regression through the origin of the relationship between the PTRS and LA.

Crop/Blocks	Linear regression code *p*-value	R^2	RMSE (m^2/m)	Linear regression through the origin	RMSE (m^2/m)
Apple / 14	y = 1.61x – 2.88 ***	0.88	1.49	y = 1.26x	1.77
Pear / 17	y = 1.62x – 2.00 ***	0.85	1.00	y = 1.35x	1.08
Vineyard / 26	y = 1.51x – 1.15 ***	0.80	0.61	y = 1.14x	0.69
All / 57	y = 1.47x – 1.18 ***	0.93	1.10	y = 1.28x	1.22

Represented in Fig. 9 and Table 3 are the linear regressions between the PTRS and the LA of the four vine varieties. As in Fig. 7, differences between them can be observed. Prudence again is required, however, as the blocks of each variety are few in number, making it difficult to reach firm conclusions. In the case of Cabernet, when the regression passes through the origin, the slope is less than 1. This means that the LA is lower than the PTRS. To understand this value, we can imagine an isolated leaf and its four projections. It is not difficult to imagine that the PTRS can be greater than its LA. Therefore, values below 1 are possible, though normally, as can be seen in Figs. 8 and 9, they will be above 1.

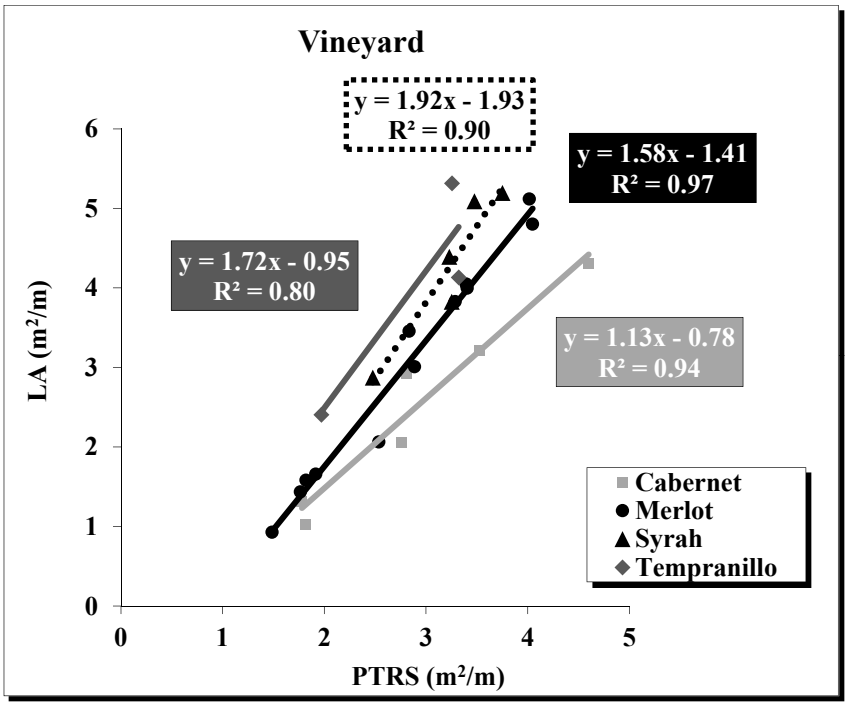

Fig. 9. Scatter diagram and linear regression of the relationship between the PTRS and LA for Cabernet, Merlot, Syrah and Tempranillo vines, fitted independently.

Table 3
Linear regression and linear regression through the origin of the relationship between the PTRS and LA.

Crop/Blocks	Linear regression code *p*-value	R^2	RMSE (m^2/m)	Linear regression through the origin	RMSE (m^2/m)
Cabernet / 6	y = 1.13x – 0.78 ***	0.94	0.27	y = 0.89x	0.37
Merlot / 12	y = 1.58x – 1.41 ***	0.97	0.22	y = 1.12x	0.46
Syrah / 5	y = 1.92x – 1.93 *	0.90	0.27	y = 1.33x	0.37
Tempranillo / 3	y = 1.72x – 0.95	0.80	0.53	y = 1.40x	0.57

The PTRS uses four projected faces (4F). An explanation is given below of how the regression models evolve when using fewer faces.

Normally, the least illuminated face is the lower one. If we eliminate the bottom projection and are left with 2PFS + 1 PTS, 3 faces in total (3F) (Table 4), it can be seen that the R^2 and RMSE of the regressions are practically the same as when 4F are used (Table 2). Logically, the slopes are greater given that LA is spread around a lower outer surface (3F). Giving less weight to the top-view projection, removing one of the faces, neither improves nor worsens the results.

Table 4
Linear regression and linear regression through the origin of the relationship between the (2PFS+1PTS) and LA.

Crop/Blocks	Linear regression code *p*-value	R^2	RMSE (m^2/m)	Linear regression through the origin	RMSE (m^2/m)
Apple / 14	y = 2.12x – 3.43 ***	0.89	1.44	y = 1.58x	1.80
Pear / 17	y = 1.89x – 1.49 ***	0.84	1.05	y = 1.64x	1.10
Vineyard / 26	y = 1.95x – 1.25 ***	0.83	0.57	y = 1.44x	0.66
All / 57	y = 1.82x – 1.16 ***	0.93	1.08	y = 1.60x	1.20

In the case of using only the PFS (Fig. 10 and Table 5), the regressions continue having a high correlation. The lowest R^2, 0.74, is for pear trees, and surprisingly it increases slightly for vine, reaching 0.85. There is no logical explanation for this increase in R^2 as it makes no sense that when ignoring the PTS the regression should improve. Having reached this point, if the regressions which pass through the origin are used, LA estimation becomes much simpler and only involves calculating the PFS and multiplying it by a factor of around 4, depending on the species.

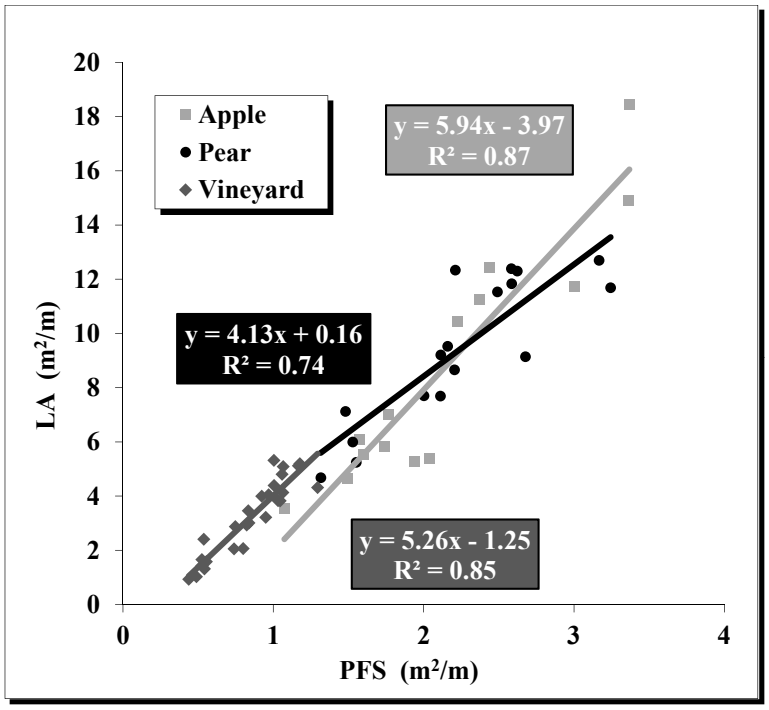

Fig. 10. Scatter diagram and linear regression of the relationship between the PFS and LA for vine, pear and apple tree blocks, fitted independently.

Table 5
Linear regression and linear regression through the origin of the relationship between the PFS and LA.

Crop/Blocks	Linear regression code *p*-value	R^2	RMSE (m^2/m)	Linear regression through the origin	RMSE (m^2/m)
Apple / 14	y = 5.94x – 3.97 ***	0.87	1.54	y = 4.26x	1.95
Pear / 17	y = 4.13x + 0.16 ***	0.74	1.33	y = 4.20x	1.33
Vineyard / 26	y = 5.26x – 1.25 ***	0.85	0.53	y = 3.90x	0.63
All / 57	y = 4.64x – 0.92 ***	0.91	1.22	y = 4.19x	1.29

In the case of only using the PTS (Fig. 11 and Table 6), the regressions for each crop are worse with respect to the previous cases with 4F, 3F and 1F(PFS). Pear trees are the crop with the worst regression, with an R^2 of 0.45. Despite everything, the set of all the blocks, without differentiation of species, provides a high correlation with R^2 = 0.80. These results suggest that with the topside point of view, for example, using a drone, LA estimation is possible.

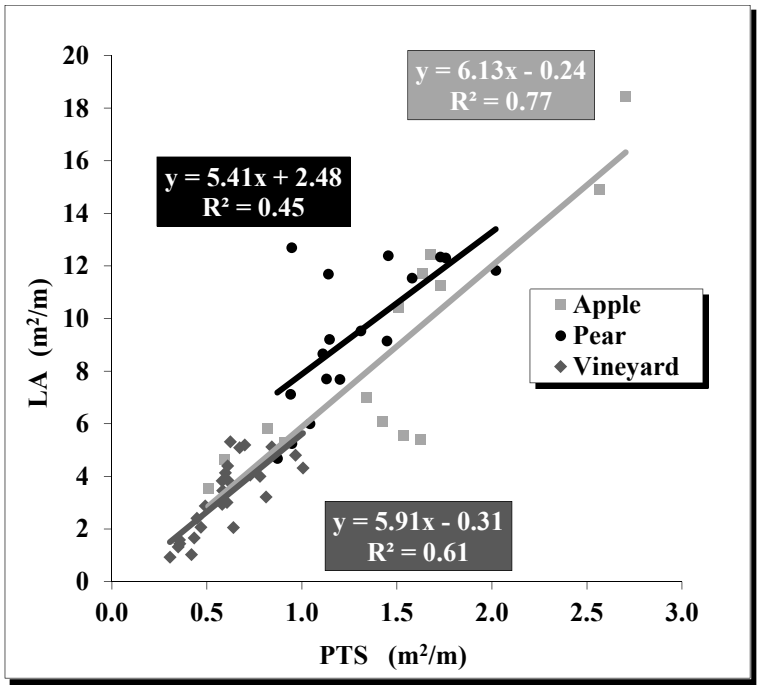

Fig. 11. Scatter diagram and linear regression of the relationship between the PTS and LA for vine, pear and apple tree blocks, fitted independently.

Table 6
Linear regression and linear regression through the origin of the relationship between the PTS and LA.

Crop/Blocks	Linear regression code *p*-value	R^2	RMSE (m^2/m)	Linear regression through the origin	RMSE (m^2/m)
Apple / 14	y = 6.13x – 0.24 ***	0.77	2.04	y = 5.98x	2.05
Pear / 17	y = 5.41x + 2.48 **	0.45	1.92	y = 7.22x	2.02
Vineyard / 26	y = 5.91x – 0.31 ***	0.61	0.87	y = 5.44x	0.87
All / 57	y = 6.65x – 0.33 ***	0.80	1.79	y = 6.40x	1.79

After analyzing the results in this section, the second working hypothesis which assumed a linear relationship between the PTRS and the LA can be confirmed. It has also been shown that there is a good linear relationship between the PFS and the LA with the advantage of it being a more easily obtainable variable than the PTRS.

3.3. Estimation of the LA from the estimated projected surfaces

The drawback of using the PFS and PTS is that they are obtained from the TRLV which, requires a LIDAR-based measurement system. This section shows the results for LA estimation based on estimation of PFS and PTS without using any LIDAR sensor. The result of comparing the PTRS and the EPTRS can be seen in Fig. 12. A very high correlation can be observed. This indicates that the errors committed in the estimation of gaps and in the calculation of depth are small with respect to the actual gaps of the point cloud. It is understandable that the human component of visual estimation could create doubts about the method, but we believe that the procedure is so simple that anybody can

obtain more than acceptable results with just a little training. Verification of this hypothesis is not contemplated among the aims of the present study.

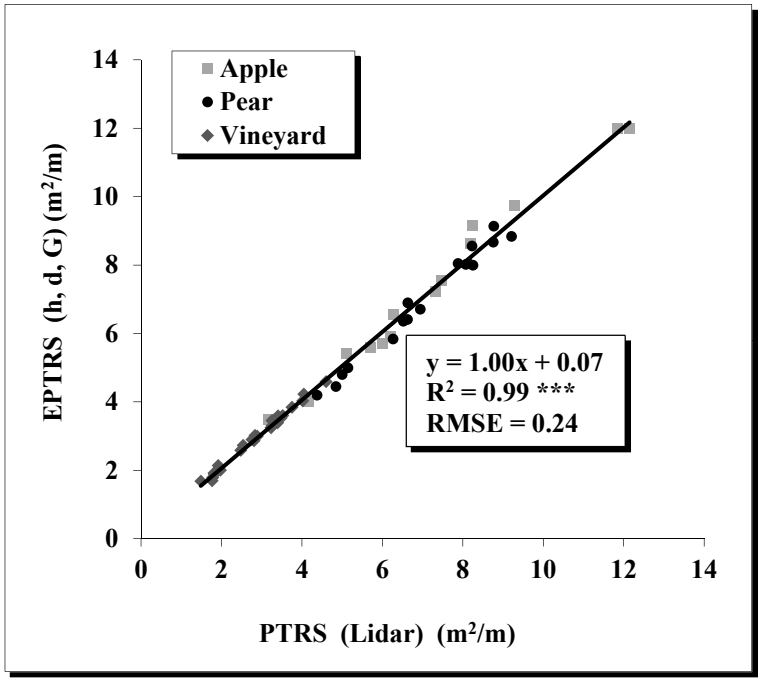

Fig. 12. Scatter diagram and linear regression of the relationship between the PTRS and EPTRS for vine, pear and apple tree blocks.

It can be seen in Fig. 13 and Table 7 that the correlation between the EPTRS and the LA continues to be very high and practically the same as in Fig. 8 with the PTRS.

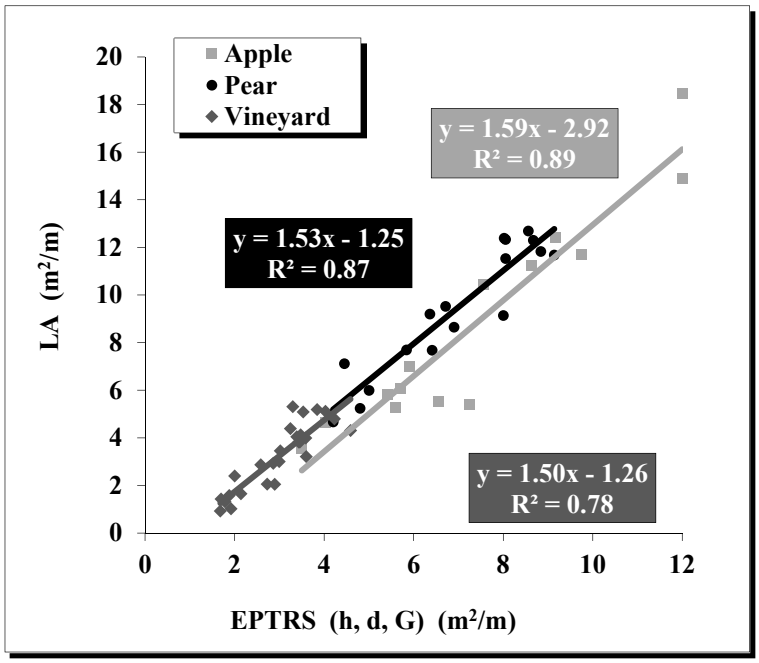

Fig. 13. Scatter diagram and linear regression of the relationship between the EPTRS and LA for vine, pear and apple tree blocks, fitted independently.

Table 7
Linear regression and linear regression through the origin of the relationship between the EPTRS and LA.

Crop/Blocks	Linear regression code *p*-value	R^2	RMSE (m^2/m)	Linear regression through the origin	RMSE (m^2/m)
Apple / 14	y = 1.59x – 2.92 ***	0.89	1.39	y = 1.23x	1.69
Pear / 17	y = 1.53x – 1.25 ***	0.87	0.93	y = 1.36x	0.97
Vineyard / 26	y = 1.50x – 1.26 ***	0.78	0.64	y = 1.11x	0.72
All / 57	y = 1.47x – 1.26 ***	0.93	1.08	y = 1.27x	1.22

It can be seen in Fig. 14 and Table 8 that the correlation between the EPFS and the LA also continues to be very high and practically the same as in Fig. 10 with the PFS. In this latter case, it should be noted that LA estimation is carried out based only on height and gap estimation. This means that just one person, armed with a measuring tape, calculator, Eq. (3) and Table 5, can estimate *in situ* the LA simply, accurately and immediately.

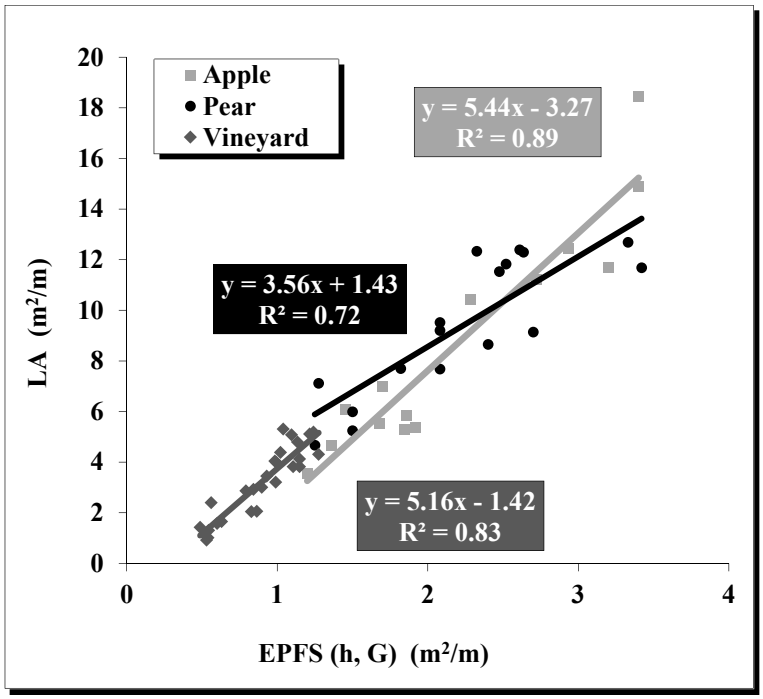

Fig. 14. Scatter diagram and linear regression of the relationship between the EPFS and LA for vine, pear and apple tree blocks, fitted independently.

Table 8
Linear regression and linear regression through the origin of the relationship between the EPFS and LA.

Crop/Blocks	Linear regression code *p*-value	R^2	RMSE (m^2/m)	Linear regression through the origin	RMSE (m^2/m)
Apple / 14	y = 5.44x – 3.27 ***	0.89	1.42	y = 4.11x	1.77
Pear / 17	y = 3.56x +1.43 ***	0.72	1.38	y = 4.16x	1.43
Vineyard / 26	y = 5.16x – 1.42 ***	0.83	0.56	y = 3.69x	0.67
All / 57	y = 4.52x – 0.90 ***	0.91	1.22	y = 4.08x	1.29

Below, an analysis is made of the relationship between the frontal surface area, without taking into account the gap fraction, and the LA. This frontal surface without gaps, if we refer to it by linear meter, it comes down to studying the relationship between the height of the blocks and the LA. It can be seen in Fig. 15 and Table 9, that the worst regression takes place for apple trees, with *p*-value>0.1. For pear trees and vines, the *p*-value is below 0.001 and the R^2 values are 0.62 and 0.54, respectively. As for the previously studied variables, the RMSE values obtained with height are the worst except for pear trees where it is the second worst (Table 10). It can be concluded from these results that the variable height alone does not explain well the LA and that calculation or estimation of the percentage of gaps is fundamental for a valid estimation.

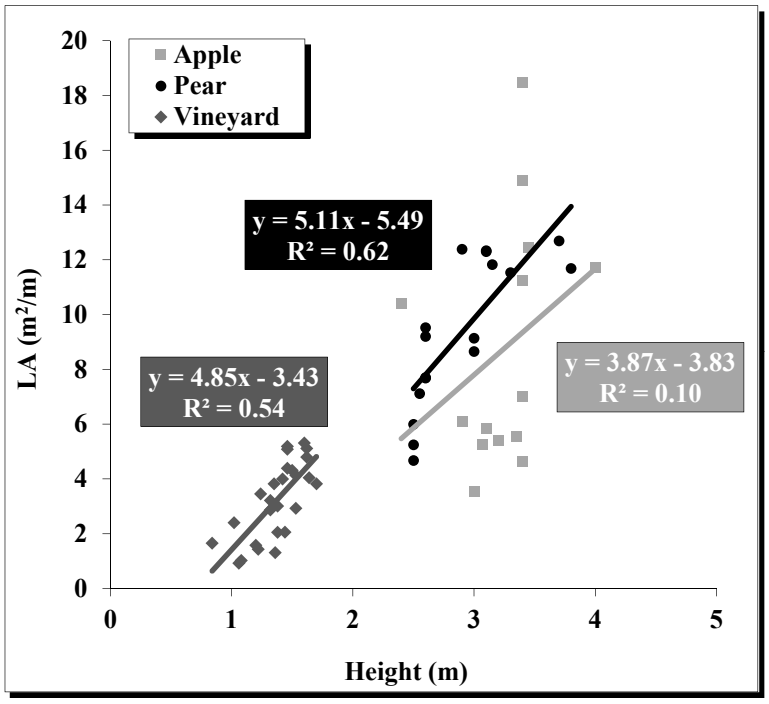

Fig. 15. Scatter diagram and linear regression of the relationship between the height of the green wall of the crop and LA for vine, pear and apple tree blocks, fitted independently.

Table 9
Linear regression and linear regression through the origin of the relationship between height and LA.

Crop/Blocks	Linear regression code *p*-value	R^2	RMSE (m^2/m)	Linear regression through the origin	RMSE (m^2/m)
Apple / 14	y = 3.87x – 3.83	0.10	4.09	y = 2.71x	4.11
Pear / 17	y = 5.11x – 5.49 ***	0.62	1.61	y = 3.26x	1.77

Vineyard / 26	y = 4.85x – 3.43 ***	0.54	0.94	y = 2.41x	1.07
All / 57	y = 3.52x – 1.65 ***	0.63	2.42	y = 2.90x	2.50

3.4. RMSE analysis for leaf area and LAI estimation.

In this section the variables used for the estimation of the LA are evaluated based on the RMSE of the obtained regressions.

Table 10

Summary of the RMSEs (m^2/m) of the regressions between the variables studied and the LA (m^2/m).

	All	Apple	Pear	Vineyard	Caber-net	Merlot	Syrah	Tempra-nillo
TRLV	1.26	1.67	1.05	0.51	0.39	0.31	0.07	0.49
PTRS/EPTRS(4F)	1.10/1.08	1.49/1.39	1.00/0.93	0.61/0.64	0.27	0.22	0.27	0.53
2PFS+PTS (3F)	1.08	1.44	1.05	0.57				
PFS/EPFS (1F)	1.22/1.22	1.54/1.42	1.33/1.38	0.53/0.56				
PTS (1F)	1.79	2.04	1.92	0.87				
Height (1F)	2.42	4.09	1.61	0.94				

Table 11

Summary of the R^2 of the regressions between the variables studied and the LA (m^2/m).

	All	Apple	Pear	Vineyard	Caber-net	Merlot	Syrah	Tempra-nillo
TRLV	0.90	0.85	0.84	0.86	0.88	0.95	0.99	0.83
PTRS/EPTRS(4F)	0.93/0.93	0.88/0.89	0.85/0.87	0.80/0.78	0.94	0.97	0.90	0.80
2PFS+PTS (3F)	0.93	0.89	0.84	0.83				
PFS/EPFS (1F)	0.91/0.91	0.87/0.89	0.74/0.72	0.85/0.83				
PTS (1F)	0.80	0.77	0.45	0.61				
Height (1F)	0.63	0.10	0.62	0.54				

All the RMSE and R^2 calculated in the LA estimation regressions are grouped together in Tables 10 and 11.

In the general case of non-differentiation of species (All), the best results are obtained when using 4F and 3F. The results obtained are also very good when based on the TRLV and the PFS/EPFS. The errors in LA estimation increase when the gap fraction is not taken into consideration (PTS and height). The worst result is obtained with the variable height. The case of apple trees is very similar to the general case described above, but with higher RMSE values and lower R^2. The value of 1.42 obtained from the EPFS is somewhat unexpected. This reduction of the RMSE with respect to the PFS (1.54) has no logical explanation. The case of pear trees also follows the general pattern with the exception that the worst result is found with the PTS and not with height. Vineyards give the best result based on the TRLV. Very good results are also obtained with 4F, 3F and PFS/EPFS. The worst result, as in the general case, is obtained from height. In the case of differentiation between varieties, the RMSEs are quite lower, except for Tempranillo. Therefore, though these fits are more accurate, prudence is required as few blocks were used for each variety, especially Tempranillo with just three blocks.

In view of all of the above, and contemplating a more accurate, faster and automatable system using LIDAR sensors, we propose as interesting variables, the TRLV, PTRS, PFS and the 2PFS+PTS combination. The small differences that exist between the regression models of these four variables and the LA are not large enough to allow a clear decision in favor of any particular one of them. If a simple, rapid and accurate system to estimate the LA and LAI *in situ* is required, we propose use of the EPFS variable as it meets these three required conditions. Finally, an analysis is made below of the relationship between the EPFS and the LAI.

Table 12
Linear regression and linear regression through the origin of the relationship between the EPFS and LAI.

Crop/Blocks	Linear regression code *p*-value	R^2	RMSE (m^2/m)	Linear regression through the origin	RMSE (m^2/m)
Apple / 14	y = 1.40x – 0.93 ***	0.89	0.36	y = 1.02x	0.47
Pear / 17	y = 1.01x + 0.01 ***	0.74	0.37	y = 1.01x	0.37
Vineyard / 26	y = 1.72x – 0.47 ***	0.83	0.19	y = 1.23x	0.22
All / 57	y = 1.02x + 0.04 ***	0.85	0.36	y = 1.04x	0.36

High correlations can be observed in Table 12 between the EPFS and the LAI. The lowest R^2 corresponds to pear trees ($R^2 = 0.74$). If we consider the regressions that pass through the origin, it can be seen that in pear and apple trees the relationship between the EPFS and the LAI is practically 1. This takes place because to change from EPFS to LA we have to multiply by a factor of approximately four (Table 8) and to convert LA into LAI we have to divide by the distance between rows, which is also approximately four (Table 1). Care needs to be taken with LAI estimation because it depends on row spacing and, therefore, this correlation of 1 is only valid for row spacing in the order of 4 m. In the case of vineyards, with row spacing of 3 m in all the blocks, the correlation between the EPFS and the LAI is 1.23.

4. Conclusions

This work is based on two hypotheses and three objectives. In the development of the first objective it has been demonstrated that the three species (apple, pear and vine) behave similarly in terms of correlation between the TRLV and the LA. The logarithmic regressions that were obtained are very significant and have R^2 values of 0.85, 0.84 and 0.86 in apple, pear and vine, respectively. With these results the first hypothesis is confirmed, which considers TRLV to be a good variable for the estimation of the LA.

In the development of the second objective very significant linear regressions have been obtained between the PTRS and the LA, with R^2 values of 0.88, 0.85 and 0.80 for apple, pear and vine, respectively. The regression lines are very close, with very similar slopes. This is surprising principally because of the morphological differences between fruit trees and vines. The similarity in results indicates that the three crops behave similarly in terms of leaf arrangement. If only one projected face is taken into account, the variable that best explains the LA is the PFS. These results confirm the second hypothesis that contemplates a linear relationship between the PTRS and the LA.

In the third objective, an alternative method is proposed for *in situ* LA estimation, without using LIDAR, based on the EPFS and the EPTS. The height of the wall of vegetation, the mean maximum depth of the crop row and a visual estimation of the gap fraction were used to obtain these variables. Doubts will assuredly arise with respect to the last of these parameters given the subjective nature of the estimation. However, prior pictogram-based training with known gap fractions can be used to mitigate this problem. The results obtained with this simplified method were very similar to those obtained with LIDAR-based methods. As the procedure is a very simple one, anybody with a brief training sessions in gap fraction estimation can make good *in situ* LA estimations using only a measuring tape and calculator.

Finally, when considering a precise, rapid and automatable system based on LIDAR sensors, we propose as interesting variables the TRLV, PTRS, PFS and the 2PFS+PTS combination. The small differences that exist between the regression models of these four variables and the LA are not large enough to allow a clear decision in favor of any particular one of them. If a simple, rapid and accurate system to estimate the LA and LAI *in situ* is required, the use of the EPFS variable is proposed since it has the three required conditions. Variables which do not take into account the gap fraction, PTS, EPTS and height, are the variables which worst explain the LA.

Acknowledgements

This research was partially funded by the Spanish Ministry of Economy and Competitiveness (projects AGL2002-04260-C04-02, AGL2007-66093-C04-03, AGL2010-22304-C04-03 and AGL2013-48297-C2-2-R) and EU FEDER. Funding of Secretaria d'Universitats i Recerca del Departament d'Empresa i Coneixement de la Generalitat de Catalunya under Grant 2017 SGR 646 is also thanked.

References

Arnó, J., Escolà, A., Masip, J., Rosell-Polo, J.R., 2015. Influence of the scanned side of the row in terrestrial laser sensor applications in vineyards: practical consequences. Precis. Agric. 16, 119–128. doi:10.1007/s11119-014-9364-7

Arnó, J., Escolà, A., Vallès, J.M., Llorens, J., Sanz, R., Masip, J., Palacín, J., Rosell-Polo, J.R., 2013. Leaf area index estimation in vineyards using a ground-based LiDAR scanner. Precis. Agric. 14, 290–306. doi:10.1007/s11119-012-9295-0

Auat Cheein, F.A., Guivant, J., Sanz, R., Escolà, A., Yandún, F., Torres-Torriti, M., Rosell-Polo, J.R., Cheein, F.A.A., Guivant, J., Sanz, R., Escolà, A., Yandún, F., Torres-Torriti, M., Rosell-Polo, J.R., 2015. Real-time approaches for characterization of fully and partially scanned canopies in groves. Comput. Electron. Agric. 118, 361–371. doi:10.1016/j.compag.2015.09.017

Ballesteros, R., Ortega, J.F., Hernandez, D., Moreno, M.A., 2015. Characterization of Vitis vinifera L. Canopy Using Unmanned Aerial Vehicle-Based Remote Sensing and Photogrammetry Techniques. Am. J. Enol. Vitic. 66, 120–129. doi:10.5344/ajev.2014.14070

Chianucci, F., Cutini, A., Corona, P., Puletti, N., 2014. Estimation of leaf area index in understory deciduous trees using digital photography. Agric. For. Meteorol. 198–199, 259–264. doi:10.1016/j.agrformet.2014.09.001

724 Cohen, S., Raveh, E., Li, Y., Grava, A., Goldschmidt, E.E., 2005. Physiological
725 responses of leaves, tree growth and fruit yield of grapefruit trees under reflective
726 shade screens. Sci. Hortic. (Amsterdam). 107, 25–35.
727 doi:10.1016/j.scienta.2005.06.004
728 De Bei, R., Fuentes, S., Gilliham, M., Tyerman, S., Edwards, E., Bianchini, N., Smith,
729 J., Collins, C., 2016. VitiCanopy: A Free Computer App to Estimate Canopy Vigor
730 and Porosity for Grapevine. Sensors 16, 585. doi:10.3390/s16040585
731 Diago, M.-P., Correa, C., Millán, B., Barreiro, P., Valero, C., Tardaguila, J., 2012.
732 Grapevine Yield and Leaf Area Estimation Using Supervised Classification
733 Methodology on RGB Images Taken under Field Conditions. Sensors 12, 16988–
734 17006. doi:10.3390/s121216988
735 Doring, J., Stoll, M., Kauer, R., Frisch, M., Tittmann, S., 2014. Indirect Estimation of
736 Leaf Area Index in VSP-Trained Grapevines Using Plant Area Index. Am. J. Enol.
737 Vitic. 65, 153–158. doi:10.5344/ajev.2013.13073
738 Du, S., Kang, S., Li, F., Du, T., 2017. Water use efficiency is improved by alternate
739 partial root-zone irrigation of apple in arid northwest China. Agric. Water Manag.
740 179, 184–192. doi:10.1016/j.agwat.2016.05.011
741 Escolà, A., Martínez-Casasnovas, J.A., Rufat, J., Arnó, J., Arbonés, A., Sebé, F.,
742 Pascual, M., Gregorio, E., Rosell-Polo, J.R., 2017. Mobile terrestrial laser scanner
743 applications in precision fruticulture/horticulture and tools to extract information
744 from canopy point clouds. Precis. Agric. 18, 111–132. doi:10.1007/s11119-016-
745 9474-5
746 Escolà, A., Planas, S., Rosell, J.R., Pomar, J., Camp, F., Solanelles, F., Gracia, F.,
747 Llorens, J., Gil, E., 2011. Performance of an Ultrasonic Ranging Sensor in Apple
748 Tree Canopies. Sensors 11, 2459–2477. doi:10.3390/s110302459
749 Fang, H., Li, W., Wei, S., Jiang, C., 2014. Seasonal variation of leaf area index (LAI)
750 over paddy rice fields in NE China: Intercomparison of destructive sampling, LAI-
751 2200, digital hemispherical photography (DHP), and AccuPAR methods. Agric.
752 For. Meteorol. 198–199, 126–141. doi:10.1016/j.agrformet.2014.08.005
753 Fernández, V., Del Río, V., Pumariño, L., Igartua, E., Abadía, J., Abadía, A., 2008.
754 Foliar fertilization of peach (Prunus persica (L.) Batsch) with different iron
755 formulations: Effects on re-greening, iron concentration and mineral composition
756 in treated and untreated leaf surfaces. Sci. Hortic. (Amsterdam). 117, 241–248.
757 doi:10.1016/j.scienta.2008.05.002
758 Fuentes, S., Poblete-Echeverría, C., Ortega-Farias, S., Tyerman, S., De Bei, R., 2014.
759 Automated estimation of leaf area index from grapevine canopies using cover
760 photography, video and computational analysis methods. Aust. J. Grape Wine Res.
761 20, 465–473. doi:10.1111/ajgw.12098
762 Hernandez-Santana, V., Fernández, J.E., Cuevas, M.V., Perez-Martin, A., Diaz-Espejo,
763 A., 2017. Photosynthetic limitations by water deficit: Effect on fruit and olive oil
764 yield, leaf area and trunk diameter and its potential use to control vegetative
765 growth of super-high density olive orchards. Agric. Water Manag. 184, 9–18.
766 doi:10.1016/j.agwat.2016.12.016
767 Jonckheere, I., Fleck, S., Nackaerts, K., Muys, B., Coppin, P., Weiss, M., Baret, F.,
768 2004. Review of methods for in situ leaf area index determination. Agric. For.
769 Meteorol. 121, 19–35. doi:10.1016/j.agrformet.2003.08.027
770 Kliewer, W.M., Dokoozlian, N.K., 2005. Leaf Area/Crop Weight Ratios of Grapevines:
771 Influence on Fruit Composition and Wine Quality. Am. J. Enol. Vitic 562, 19–23.
772 Liu, C., Kang, S., Li, F., Li, S., Du, T., 2013. Canopy leaf area index for apple tree
773 using hemispherical photography in arid region. Sci. Hortic. (Amsterdam). 164,

610–615. doi:10.1016/j.scienta.2013.10.009
Liu, J., Pattey, E., Admiral, S., 2013. Assessment of in situ crop LAI measurement using unidirectional view digital photography. Agric. For. Meteorol. 169, 25–34. doi:10.1016/j.agrformet.2012.10.009
Llop, J., Gil, E., Llorens, J., Miranda-Fuentes, A., Gallart, M., 2016. Testing the Suitability of a Terrestrial 2D LiDAR Scanner for Canopy Characterization of Greenhouse Tomato Crops. Sensors 16, 1435. doi:10.3390/s16091435
Llorens, J., Gil, E., Llop, J., Escolà, A., 2011a. Ultrasonic and LIDAR Sensors for Electronic Canopy Characterization in Vineyards: Advances to Improve Pesticide Application Methods. Sensors 11, 2177–2194. doi:10.3390/s110202177
Llorens, J., Gil, E., Llop, J., Queraltó, M., 2011b. Georeferenced LiDAR 3D Vine Plantation Map Generation. Sensors 11, 6237–6256. doi:10.3390/s110606237
Méndez, V., Catalá N, H., Rosell-Polo, J.R., Arnó, J., Sanz, R., Catalán, H., Rosell-Polo, J.R., Arnó, J., Sanz, R., 2013. LiDAR simulation in modelled orchards to optimise the use of terrestrial laser scanners and derived vegetative measures. Biosyst. Eng. 115, 7–19. doi:10.1016/j.biosystemseng.2013.02.003
Moorthy, I., Miller, J.R., Hu, B., Chen, J., Li, Q., 2008. Retrieving crown leaf area index from an individual tree using ground-based lidar data. Can. J. Remote Sens. 34, 320–332. doi:10.5589/m08-027
Mora, M., Avila, F., Carrasco-Benavides, M., Maldonado, G., Olguín-Cáceres, J., Fuentes, S., 2016. Automated computation of leaf area index from fruit trees using improved image processing algorithms applied to canopy cover digital photograpies. Comput. Electron. Agric. 123, 195–202. doi:10.1016/j.compag.2016.02.011
Palmer, J.W., Avery, D.J., Wertheim, S.J., 1992. Effect of apple tree spacing and summer pruning on leaf area distribution and light interception. Sci. Hortic. Elsevier Sci. Publ. B.V 52, 303–312.
Pascuzzi, S., Cerruto, E., Manetto, G., 2017. Foliar spray deposition in a “tendone” vineyard as affected by airflow rate, volume rate and vegetative development. Crop Prot. 91, 34–48. doi:10.1016/j.cropro.2016.09.009
Pereira, A.R., Green, S.R., Nova, N.A.V., 2007. Sap flow, leaf area, net radiation and the Priestley–Taylor formula for irrigated orchards and isolated trees. Agric. Water Manag. 92, 48–52. doi:10.1016/j.agwat.2007.01.012
Pfeiffer, S.A., Guevara, J., Cheein, F.A., Sanz, R., 2018. Mechatronic terrestrial LiDAR for canopy porosity and crown surface estimation. Comput. Electron. Agric. 146, 104–113. doi:10.1016/j.compag.2018.01.022
Planas, S., Camp, F., Escolà, A., Solanelles, F., Sanz, R., Rosell, J.R., 2013. Advances in pesticide dose adjustment in tree crops. Proc. Precis. Agric. 13. 533–539. doi:10.3920/987-90-8686-778-3
Poblete-Echeverría, C., Fuentes, S., Ortega-Farias, S., Gonzalez-Talice, J., Yuri, J.A. ntonio, 2015. Digital cover photography for estimating leaf area index (LAI) in apple trees using a variable light extinction coefficient. Sensors (Basel). 15, 2860–2872. doi:10.3390/s150202860
Rosell, J.R., Llorens, J., Sanz, R., Arnó, J., Ribes-Dasi, M., Masip, J., Escolà, A., Camp, F., Solanelles, F., Gràcia, F., Gil, E., Val, L., Planas, S., Palacín, J., 2009. Obtaining the three-dimensional structure of tree orchards from remote 2D terrestrial LIDAR scanning. Agric. For. Meteorol. 149, 1505–1515. doi:10.1016/j.agrformet.2009.04.008
Rosell, J.R., Sanz, R., 2012. A review of methods and applications of the geometric characterization of tree crops in agricultural activities. Comput. Electron. Agric.

824 81, 124–141. doi:10.1016/j.compag.2011.09.007
825 Rosell Polo, J.R., Sanz, R., Llorens, J., Arnó, J., Escolà, A., Ribes-Dasi, M., Masip, J.,
826 Camp, F., Gràcia, F., Solanelles, F., Pallejà, T., Val, L., Planas, S., Gil, E., Palacín,
827 J., 2009. A tractor-mounted scanning LIDAR for the non-destructive measurement
828 of vegetative volume and surface area of tree-row plantations: A comparison with
829 conventional destructive measurements. Biosyst. Eng. 102, 128–134.
830 doi:10.1016/j.biosystemseng.2008.10.009
831 Sanz-Cortiella, R., Llorens-Calveras, J., Escolà, A., Arnó-Satorra, J., Ribes-Dasi, M.,
832 Masip-Vilalta, J., Camp, F., Gràcia-Aguilá, F., Solanelles-Batlle, F., Planas-
833 Demartí, S., Pallejà-Cabré, T., Palacin-Roca, J., Gregorio-Lopez, E., Del-Moral-
834 Martínez, I., Rosell-Polo, J.R., 2011. Innovative LIDAR 3D dynamic measurement
835 system to estimate fruit-tree leaf area. Sensors 11. doi:10.3390/s110605769
836 Sanz, R., Rosell, J.R.R., Llorens, J., Gil, E., Planas, S., 2013. Relationship between tree
837 row LIDAR-volume and leaf area density for fruit orchards and vineyards obtained
838 with a LIDAR 3D Dynamic Measurement System. Agric. For. Meteorol. 171–172,
839 153–162. doi:10.1016/j.agrformet.2012.11.013
840 Siegfried, W., Viret, O., Huber, B., Wohlhauser, R., 2007. Dosage of plant protection
841 products adapted to leaf area index in viticulture. Crop Prot. 26, 73–82.
842 doi:10.1016/j.cropro.2006.04.002
843